

Subtype-Specific *FBXW7* Mutation and *MYCN* Copy Number Gain in Wilms' Tumor

Richard D. Williams¹, Reem Al-Saadi¹, Tasnim Chaghtai¹, Sergey Popov¹, Boo Messahel¹, Neil Sebire², Manfred Gessler³, Jenny Wegert³, Norbert Graf⁴, Ivo Leuschner⁵, Mike Hubank², Chris Jones¹, Gordan Vujanic⁶, Kathy Pritchard-Jones¹, Children's Cancer and Leukaemia Group, and SIOP Wilms' Tumour Biology Group

Abstract

Purpose: Wilms' tumor (WT), the most common pediatric renal malignancy, is associated with mutations in several well-characterized genes, most notably *WT1*, *CTNNB1*, *WTX*, and *TP53*. However, the majority of cases do not harbor mutations in these genes. We hypothesized that additional drivers of tumor behavior would be contained within areas of consistent genomic copy number change, especially those associated with the WT risk groups defined by the International Society of Paediatric Oncology (SIOP).

Experimental Design: We analyzed high-resolution (Affymetrix 250K single nucleotide polymorphism array) genomic copy number profiles of over 100 tumors from selected risk groups treated under the SIOP protocols, further characterizing genes of interest by sequencing, Multiplex Ligation-dependent Probe Amplification, or fluorescence *in situ* hybridization.

Results: We identified *FBXW7*, an E3 ubiquitin ligase component, as a novel Wilms' tumor gene, mutated or deleted in ~4% of tumors examined. Strikingly, 3 of 14 (21%) of tumors with epithelial type histology after neoadjuvant chemotherapy had *FBXW7* aberrations, whereas a fourth WT patient had germline mutations in both *FBXW7* and *WT1*. We also showed that *MYCN* copy number gain, detected in 9 of 104 (8.7%) of cases, is relatively common in WT and significantly more so in tumors of the high risk diffuse anaplastic subtype (6 of 19, 32%).

Conclusions: Because *MYCN* is itself a target of *FBXW7*-mediated ubiquitination and degradation, these results suggest that a common pathway is dysregulated by different mechanisms in various WT subtypes. Emerging therapies that target *MYCN*, which is amplified in several other pediatric cancers, may therefore be of value in high risk Wilms' tumor. *Clin Cancer Res*; 16(7); 2036–45. ©2010 AACR.

Wilms' tumor (WT) is the most common pediatric renal malignancy. Somatic or germline mutations in several genes have been identified in WT over the last two decades. *WT1*, which encodes a zinc finger nucleic acid-binding protein with multiple roles in gene regulation and development, is mutated or deleted in ~15% of WTs (reviewed in ref. 1). Gain-of-function mutations

in WNT signaling component *CTNNB1* (β catenin) are found in a similar proportion of tumors (2), usually in combination with *WT1* mutations (3–6). Mutation or loss of a third gene, *WTX* (*FAM123B*), occurs in up to 30% of sporadic WTs (7), independently of other aberrations (8). Epigenetic abnormalities at 11p15, affecting expression of *H19* and *IGF2*, are found in significant numbers of WTs, including those cases associated with Beckwith-Wiedemann syndrome (9, 10). Increased WT incidence has also been linked with several other rare developmental disorders, some of which have defined genetic lesions that are occasionally found in sporadic tumors (11). *TP53* mutations are largely restricted to the relatively uncommon anaplastic WT subtype (12). Taken together, however, somatic mutations in known WT genes account for fewer than half of cases, and identifying the underlying drivers of the remainder is a problem of significant biological and therapeutic interest.

We have analyzed copy number aberrations in samples from the International Society of Paediatric Oncology (SIOP) 2001 WT clinical trial and study, aiming to identify novel changes associated with particular histologic

Authors' Affiliations: ¹Section of Paediatric Oncology, Institute of Cancer Research, Sutton, Surrey, United Kingdom; ²UCL Institute of Child Health, London, United Kingdom; ³University of Wuerzburg, Biocenter, Developmental Biochemistry, Am Hubland, Wuerzburg, Germany; ⁴University Hospital of the Saarland, Homburg, Germany; ⁵Institute of Pathology, University Hospital of Schleswig-Holstein, Campus Kiel, Michaelisstrasse 11, Kiel, Germany; and ⁶Department of Pathology, Cardiff University School of Medicine, Cardiff, United Kingdom

Note: Supplementary data for this article are available at Clinical Cancer Research Online (<http://clincancerres.aacrjournals.org/>).

Corresponding Author: Kathy Pritchard-Jones, Section of Paediatric Oncology, Institute of Cancer Research, 15 Cotswold Road, Sutton, Surrey SM2 5NG, United Kingdom. Phone: 44-0-20-8661-3498; Fax: 44-0-20-8661-3617; E-mail: Kathy.Pritchard-Jones@icr.ac.uk.

doi: 10.1158/1078-0432.CCR-09-2890

©2010 American Association for Cancer Research.

Translational Relevance

Wilms' tumors (WT) treated with preoperative chemotherapy according to SIOP protocols are classified by histologic subtype at resection. This reflects *in vivo* chemosensitivity and predicts subsequent prognosis but has a poorly defined molecular basis. We have identified *FBXW7* as a new Wilms' tumor gene, mutations of which are associated with epithelial type (intermediate risk) tumor histology, and have shown that copy number gain of *MYCN* is associated with anaplastic (high risk) histology. *FBXW7* mediates degradation of *MYCN*, whose overexpression at the protein level is linked with poor outcome in WT. Hence, these results implicate a common oncogenic pathway that could be targeted by new therapeutic agents, such as those being developed to inhibit *MYCN* function in neuroblastoma. Because anaplastic WT, in its metastatic or recurrent form, remains largely intractable to current therapies, the identification of a potential target associated with this histology is of high clinical relevance.

subtypes and clinical risk groups, or affecting loci of general relevance to WT. Patients in this study typically receive a short period (4-6 weeks) of neoadjuvant chemotherapy before surgery, with risk groups defined by histology at nephrectomy, a direct measure of *in vivo* chemosensitivity (13). Our analysis has now detected recurrent focal aberrations targeting two genes whose dysregulation is pathogenic in other cancers. *FBXW7*, a ubiquitin ligase component that acts as a tumor suppressor, is frequently mutated in cholangiocarcinoma and T-cell acute lymphoblastic leukemia, and somewhat less commonly in a range of other malignancies (14). Here, we identify *FBXW7* as a novel Wilms' tumor gene, which is deleted or mutated in ~4% of the tumors examined and in which the aberrations thus far detected are restricted to tumors with intermediate risk histologies. *MYCN*, a MYC family transcription factor and proto-oncogene, is amplified in neuroblastoma (15), in which it is an established biomarker for treatment stratification (reviewed in refs. 16, 17), and in several other embryonal pediatric tumors. We show that genomic gain or amplification of *MYCN*, previously described in only a few individual WT cases, is relatively common, especially in tumors of the high-risk anaplastic subtype. Because both genes are linked by a common regulatory pathway, these results may have broader implications for the mechanisms of tumorigenesis in WT.

Materials and Methods

Frozen tumor material obtained from postchemotherapy nephrectomy specimens was collected from 104 patients treated in the SIOP WT 2001 clinical trial at UK

($n = 85$) and German ($n = 19$) centers. Because the availability of suitable frozen material that meets quality control standards for array analysis depends on multiple factors, including the pathology practices at each clinical center, samples were not consecutive within the trial or by histologic risk group. A pragmatic approach to sample selection was taken, based on ensuring that approximately equal numbers of tumors in each of the major histologic groups of the SIOP 2001 classification (13) were represented (see Supplementary Data), resulting in a sample series enriched in some of the rarer subtypes. These samples were supplemented by five tumors from other sources in the *FBXW7* sequencing analysis only. Patient consent and ethical approval were obtained for the use of all samples. A section from each sample was reviewed by a pediatric pathologist to confirm tumor content without significant contamination by normal tissue. DNA was extracted from frozen material by standard protocols and was profiled at UCL Genomics on the Affymetrix Human Mapping 250K Nsp single nucleotide polymorphism (SNP) array according to the manufacturer's instructions. Data were processed for copy number estimation using the Affymetrix CNAT 4.0 package, with quantile normalization and a 0.1-Mb Gaussian smoothing window. Normal control data from the 30 Caucasian CEPH trio mothers (<http://www.cephb.fr>) was obtained from the HapMap consortium (<http://www.hapmap.org/>) and was used as the baseline for copy number comparisons. The copy number data set was processed and annotated for downstream analysis with custom Perl scripts (Available from http://www.icr.ac.uk/research/research_sections/paediatric_oncology/) and visualized in CGH Explorer (ref. 18; <http://www.ifi.uio.no/bioinf/Projects/CGHExplorer>). Data were processed for inferred loss of heterozygosity analysis with dChip (ref. 19; <http://biosun1.harvard.edu/complab/dchip/>).

The *FBXW7*, *WT1*, and *WTX* coding sequences, and the *CTNNB1* exon 3 sequence were amplified from tumor samples by standard methods (see Supplementary Data for primers). Unidirectional sequencing using one primer from each pair and the Applied Biosystems BigDye system was used for initial mutation detection; all candidate mutations were confirmed by bidirectional sequencing.

The Kreatech Poseidon MYCN (2p24) & LAF (2q11) fluorescence *in situ* hybridization probe set (Kreatech Diagnostics) was used to detect MYCN copy number with reference to the LAF locus (control) according to the manufacturer's instructions. The P252-NB Multiplex Ligation-dependent Probe Amplification (MLPA) kit (MRC-Holland) was used to measure MYCN copy number by the NHS Northern Genetics Service, Newcastle upon Tyne.

For detailed examination of histology, formalin-fixed, paraffin-embedded tissue sections were prepared and stained with H&E by standard methods.

Results

Deletion of *FBXW7* in WT. Analysis of the Affymetrix copy number data (104 tumors) revealed two samples with

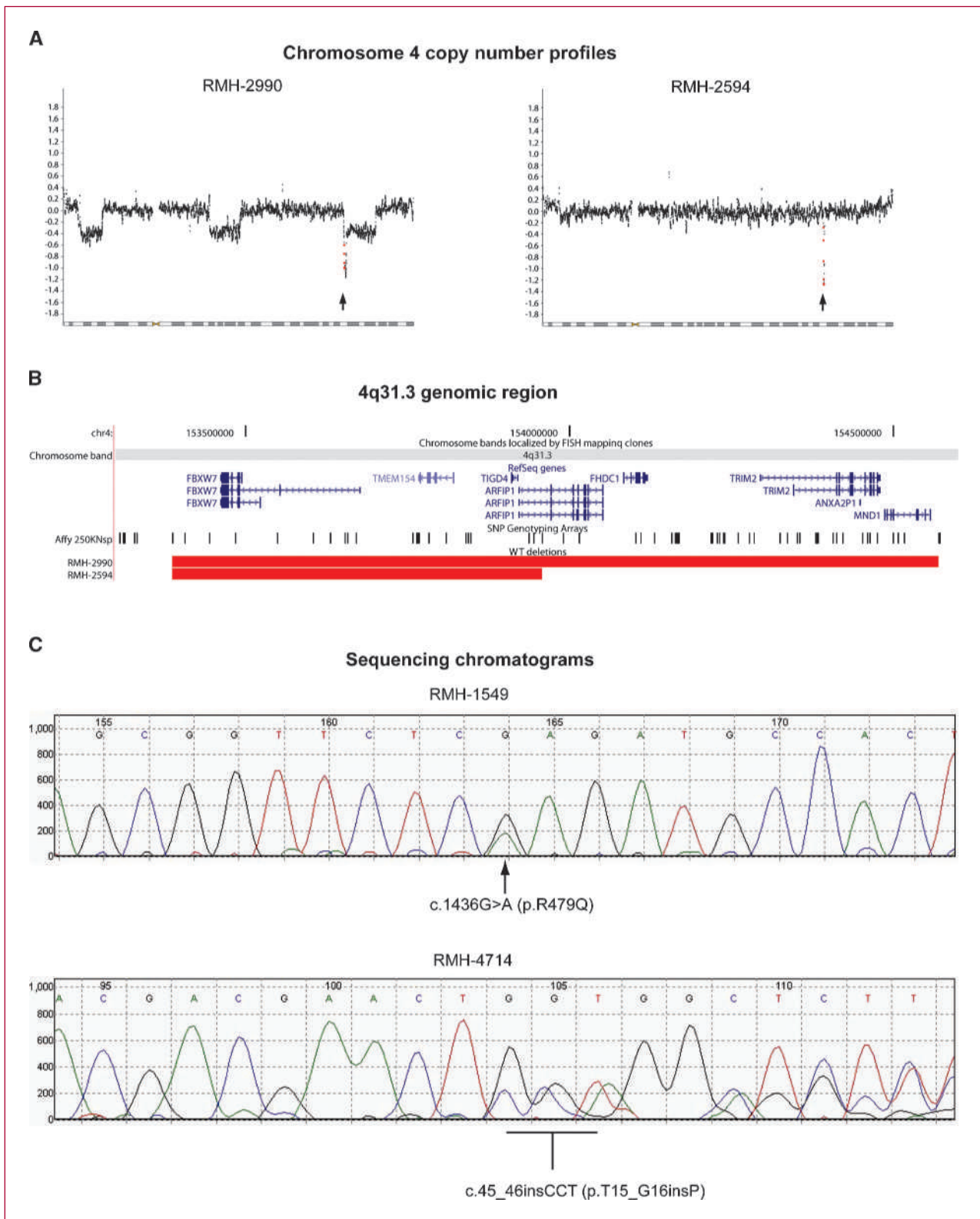


Fig. 1. *FBXW7* mutations in WT. A, chromosome 4 copy number profiles (log₂ scale) for WT samples RMH-2990 and RMH-2594. Arrow, position of the *FBXW7* gene; red, *FBXW7*-specific probe positions. B, extent of the 4q31.3 deletions relative to NCBI RefSeq genes and Affymetrix 250K SNP probe positions (48). C, sequence chromatograms for *FBXW7* mutations detected in WT samples RMH-1549 and RMH-4714; FISH, fluorescence *in situ* hybridization.

focal and apparently homozygous deletions on 4q31.1 (Fig. 1A). In both samples, loss of 1p and gain of 1q were also observed. In one case (RMH-2594) the 4q31.1 deletion was the sole additional major abnormality detected in the genome at the resolution of the 250K Nsp array. In the second (RMH-2990), three further less focal aberrations consistent with heterozygous deletions were detected on chromosome 4, but no other major genomic changes were apparent. The focal 4q31.1 deletions in both samples contained the complete sequence of the *FBXW7* gene. Although the focal aberration in RMH-2990 encompassed seven other RefSeq genes (Fig. 1B), the more limited deletion in RMH-2594 (Fig. 1B) included only two complete genes (*TMEM154* and *TIGD4*) and part of a third (*ARFIP1*) in addition to *FBXW7*. As *FBXW7* is a well-characterized tumor suppressor gene (14), whereas *TMEM154*, *TIGD4*, and *ARFIP1* have no established roles in cancer, we prioritized *FBXW7* for further evaluation.

Point mutation of *FBXW7* in WT. To determine if *FBXW7* in WT is subject to point mutations or other abnormalities below the resolution of the Affymetrix 250K array, we sequenced the coding sequence of this gene in 88 samples, 77 of which had also been analyzed on the array. All sequences were complete except in seven cases, in which data were not obtained for 1 or 2 of the 13 coding exons (see Supplementary Data). Two further mutants were detected (Fig. 1C), in both cases in tumors with neutral copy number profiles (no major changes detected; data not shown). In RMH-1549, a heterozygous G to A transition (c.1436G>A, relative to the α isoform) results in the substitution of Arg-479 with Gln (p.R479Q). Arg-479 is the second most common mutational hotspot in *FBXW7* across a range of tumor types and retention of the wild-type allele is typical of primary tumors harboring such mutations (14). In RMH-4714, a heterozygous three base insertion (c.45_46insCCT; Fig. 1C) introduces a proline at residue 16 (T15_G16insP) of the predominant *FBXW7* α isoform, a mutation previously observed in prostate cancer (14).

Sequencing *FBXW7* in matched peripheral blood DNA from the patients with tumors RMH-1549 and RMH-4714 revealed that the mutation in RMH-1549 was confined to the tumor, whereas the proline insertion in RMH-4714 was also present in the germline. It is also notable that both tumors with *FBXW7* deletions detected on the array (RMH-2594 and RMH-2990) and the sample with the Arg-479 hotspot mutation (RMH-1549) were of the relatively uncommon epithelial subtype, found in only 10% of the WTs classified according to the SIOP criteria for tumors resected after chemotherapy (13). This subtype is considered "intermediate risk." Because only 14 of 77 of the jointly arrayed and sequenced samples were epithelial type, this result suggests that *FBXW7* mutations exhibit specificity to this subtype ($P = 0.018$, Fisher's exact test). The germline proline insertion (RMH-4714) was in a patient with stromal type histology, an intermediate risk subtype frequently asso-

ciated with *WT1* and *CTNNB1* mutations (20–23). No *FBXW7* aberrations were detected in tumors with high-risk histologies or in the mixed or regressive intermediate risk subtypes.

MYCN gain in WT. Nine samples had evidence of *MYCN* gain (examples in Fig. 2A, extent of gain in Fig. 2B). In six of these tumors, this was a focal (typically ~0.25 Mb) low-copy number event (typically consistent with single copy gain). In two cases (RMH-2969 and RMH-4718) a somewhat higher level, but still focal, gain was observed. In the remaining sample (RMH-2967), a broader, high-level amplification (>10 copies) was detected and confirmed by fluorescence *in situ* hybridization in 90 of 94 assessed nuclei of cells from a frozen tumor touch preparation (Fig. 2C). The level of gain in eight of the nine samples was assessed by MLPA, which confirmed the array results (Fig. 2D). Six of the nine samples, including those with the highest levels of gain, were of the high-risk diffuse anaplastic subtype. One other tumor (RMH-3725) was also classed as a high-risk histology (blastemal type). The remaining samples (RMH-205, RMH-4644) were of intermediate risk mixed histology. Because only 19 of 104 of the tumors profiled were of the diffuse anaplastic subtype, and 6 of these (32%) had *MYCN* gain, these results indicate a significant association between anaplasia and this aberration ($P = 0.001$, Fisher's exact test).

Status of known WT genes in samples with *FBXW7* or *MYCN* aberrations. To determine if other known WT genes are mutated in the samples with *FBXW7* or *MYCN* aberrations, we examined the coding sequences of *WT1* and *WTX*, and the exon 3 sequence of *CTNNB1*, in all four samples with *FBXW7* deletion or mutation and in eight of the nine samples with *MYCN* gain; sequence data were not available for RMH-3725 (see Supplementary Data). The SNP data for all 13 samples of interest were also examined for inferred loss of heterozygosity (tumor only, without reference to matched normal; ref. 19) at 11p13 and 11p15.5.

RMH-4714, the sample with a germline *FBXW7* mutation, was found to have mutations in both *WT1* and *CTNNB1*; no other *WT1*, *CTNNB1*, or *WTX* mutations were detected in this sample series. Two heterozygous *WT1* mutations were found in RMH-4714: c.948_949insG, a single base insertion that introduces a frameshift in exon 2, and c.1568C>T (p.R390X, relative to the longest *WT1* isoform translated from the ATG initiation codon at c.401), a single base substitution that introduces a stop codon in exon 9, terminating the protein in its third zinc finger and eliminating the fourth and final zinc finger. The c.1568C>T (p.R390X) mutation was also found in the germline, but c.948_949insG was confined to the tumor, potentially representing a second hit in the other allele (allelic specificity was not determined). Two *CTNNB1* nucleotides were heterozygously mutated in RMH-4714 (tumor only), substituting adjacent amino acid residues: c.398C>G (p.P44A) and c.401T>C (p.S45P). Ser-45 is a mutational hotspot in WT and other tumors, while simultaneous P44A and S45P substitutions have

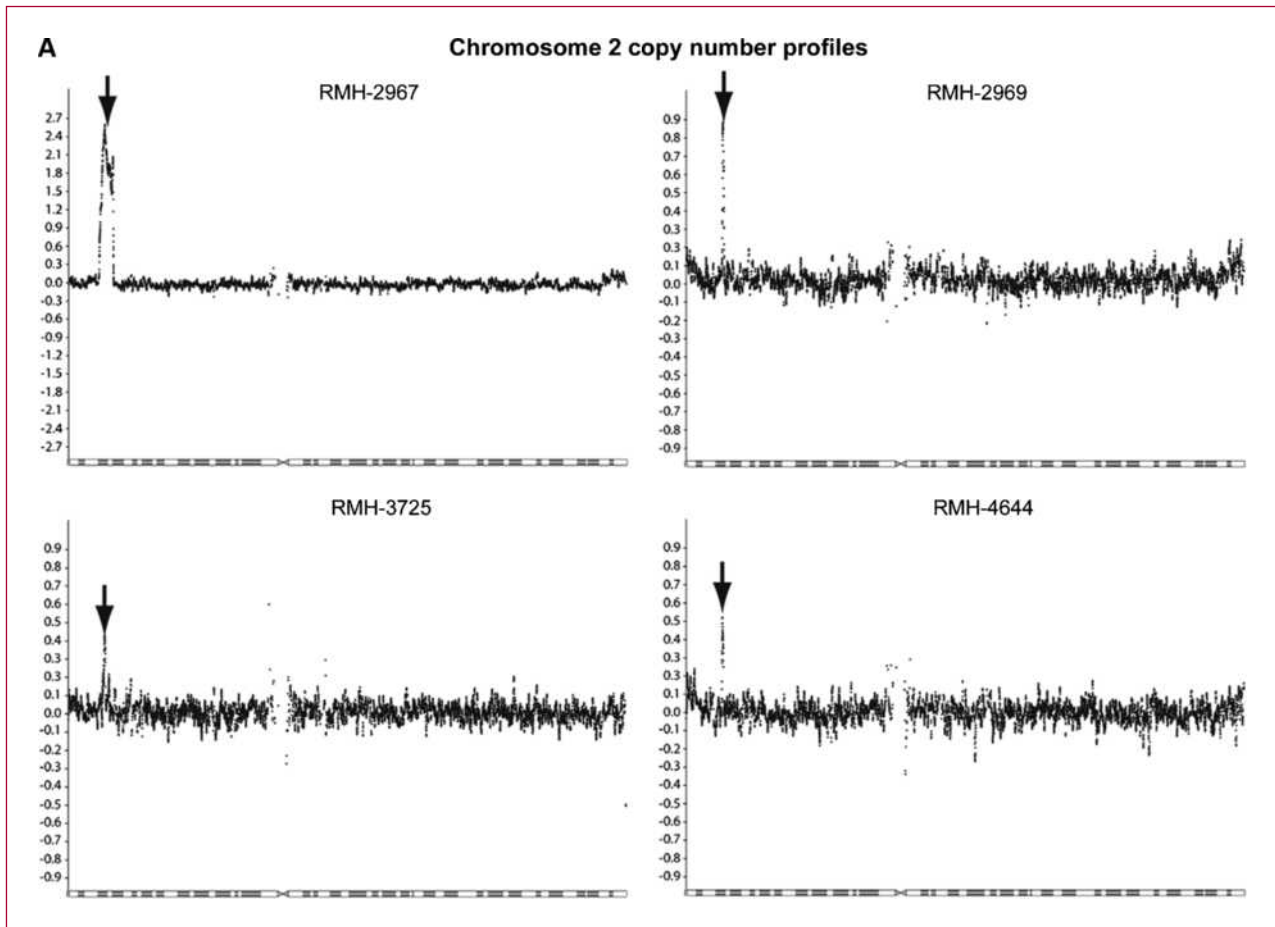


Fig. 2. *MYCN* gain in WT. A, chromosome 2 copy number profiles (\log_2 scale) for four examples of WT with gain at the *MYCN* locus. Arrow, position of the *MYCN* gene.

been reported in WT and hepatocellular carcinoma (24, 25). RMH-1549 had evidence of loss of heterozygosity at 11p15.5, but not 11p13; none of the other 12 samples had inferred loss of heterozygosity in either of these regions.

Because the patient with tumor RMH-4714 carried germline mutations in both *FBXW7* and *WT1*, we reviewed the clinical data for this case. Although not diagnosed with any known WT-associated syndrome or genitourinary abnormalities, the patient (a phenotypic and genetic XX female) had a younger than average age at diagnosis (14 months) and presented with bilateral renal masses, both features suggestive of genetic predisposition. The larger mass (11-cm diameter) proved to be a WT (RMH-4714). The smaller mass (2-cm diameter) in the contralateral kidney showed pronounced cystic change after chemotherapy; hence, it could not be confirmed whether this may have been a WT precursor lesion (nephrogenic rest).

Histology of samples with *FBXW7* or *MYCN* aberrations. Because *FBXW7* mutations were associated with epithelial histology and *MYCN* gain was associated with diffuse an-

aplasia, we reviewed the pathology reports and (where available) formalin-fixed, paraffin-embedded sections of the UK Children's Cancer and Leukaemia Group samples with aberrations in either gene to determine if they had specific distinguishing features in addition to those that defined their histologic subtypes (see Supplementary Data). All three samples with *FBXW7* aberrations, but no mutations in other WT genes (RMH-1549, RMH-2594, RMH-2990), had unambiguous epithelial-type histology (e.g., Fig. 3A and B), consisting of 90% to 100% epithelial elements (tubules with a range of differentiation and tubulo-papillary structures). No specific features beyond those normally associated with epithelial-type histology were observed, although RMH-1549, the sample with a mutation at the R479Q hotspot, was more highly differentiated than the other two tumors. RMH-4714, the sample with mutations in *WT1*, *CTNNB1*, and *FBXW7*, was clearly of stromal type histology (~85% stromal elements), although some epithelial elements (~12.5%) were detectable (data not shown). All six tumors with *MYCN* gain and diffuse anaplasia were confirmed to have the characteristic features of anaplastic

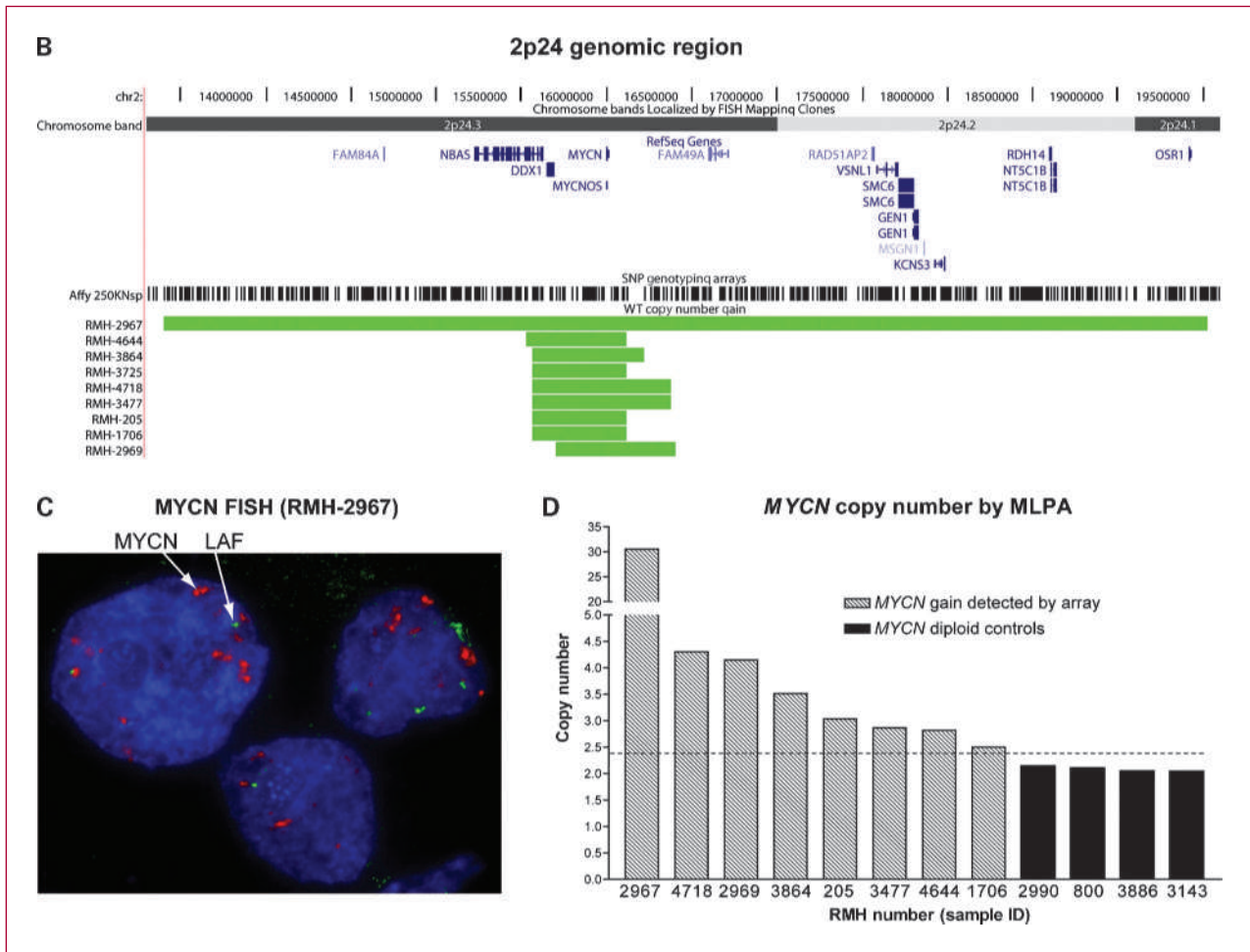


Fig. 2. Continued. B, extent of the 2p24.3 gains relative to NCBI RefSeq genes and Affymetrix 250K SNP probe positions (48). C, *MYCN* amplification (red) detected by fluorescence *in situ* hybridization with reference to LAF copy number control on 2q (green). D, *MYCN* copy number measured by MLPA (mean of two different *MYCN*-specific probes, linear scale) for eight samples with gain detected by the Affymetrix array and four control samples without 2p24.3 aberrations in their array profiles. A copy number of 2.4 (1.2× diploid) was taken as the threshold of gain (dashed line).

WT, including nuclear enlargement, hyperchromasia, and atypical mitotic figures (Fig. 3C and D). However, the tumor with the highest level of *MYCN* gain, RMH-2967, also had some areas of rhabdoid-like features, including vesicular nuclei, very prominent nucleoli, and noncohesive cells (Fig. 3C and E). Similar but less prominent features were also evident in three of the remaining five *MYCN*+ anaplastic WTs (e.g., Fig. 3D and F), but in only one of six UK anaplastic tumors without *MYCN* gain.

Discussion

FBXW7 mutations have not previously been described in WT. However, both point mutations detected here have been observed in other tumors. Arg-479 is a key surface residue in the *FBXW7* WD40 repeat III, a component of the β -propeller structure responsible for substrate recognition and a frequent mutational hotspot in

multiple tumor types (14). As in our cases, primary tumors with *FBXW7* point mutations typically retain the wild-type allele (14). Such heterozygous mutants, in which substrate binding is disrupted while other interactions remain unaffected, are believed to act through haplo-insufficient (26) or dominant-negative (27) mechanisms, and there is direct evidence that R479Q has dominant-negative activity (14).

The T15_G16insP insertion has previously been reported in a single prostate tumor, functionally tested in an embryonic kidney cell line system and found to abolish nuclear localization of the protein and its binding to a known substrate, CCNE1 (Cyclin E; ref. 14). Although the potential dominant-negative activity of the mutant protein was not assessed, it retained the ability to interact with known cofactors, a property consistent with a dominant-negative mechanism of action. The minor β and γ *FBXW7* isoforms would not be affected by this insertion, but

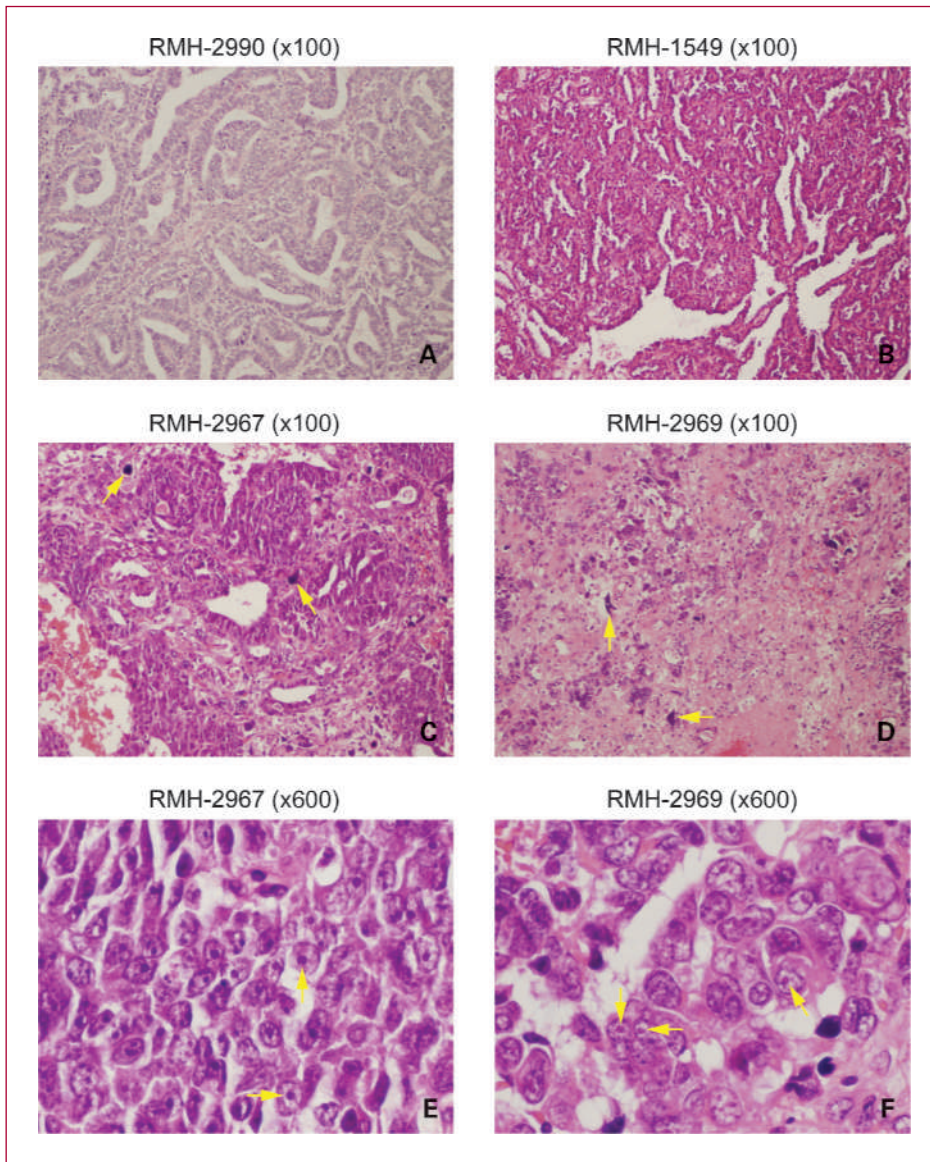


Fig. 3. H&E-stained paraffin-embedded sections showing histology of tumors with *FBXW7* or *MYCN* aberrations. A, RMH-2990 (x100 magnification). Epithelial type WT showing poorly and moderately differentiated tubules with some papillary structures. B, RMH-1549 (x100). Epithelial type WT showing highly differentiated tubules. C, RMH-2967 (x100). Diffuse anaplastic WT; arrows, examples of anaplastic cells. D, RMH-2969 (x100). Diffuse anaplastic WT; arrows, examples of anaplastic cells. E, RMH-2967 (x600). Diffuse anaplastic WT with areas of rhabdoid-like histology including prominent nucleoli (arrows). F, RMH-2969 (x600). Diffuse anaplastic WT with areas of rhabdoid-like histology including prominent nucleoli (arrows).

neither has the ability to localize to the nucleoplasm and interact with nuclear substrates such as Cyclin E even in the wild-type form and so could not compensate for the mutation. Although T15_G16insP in RMH-4714 is a germline mutation, the functional data, together with the evolutionary conservation of adjacent T15 and G16 residues in most vertebrate species from primates to *Fugu* (data not shown), strongly suggest a deleterious mutation rather than a rare polymorphism; no insertions at this position have been reported in the National Center for Biotechnology Information (NCBI) dbSNP (build 130).

FBXW7, as an important tumor suppressor gene, is likely to be the primary and potentially sole significant target of the focal homozygous deletions in RMH-2594 and RMH-2990. Similar aberrations are found in T-cell acute

lymphoblastic leukemia, a tumor type with a high frequency of *FBXW7* point mutations. Our analysis of a published series of 50 T-cell acute lymphoblastic leukemia Affymetrix SNP arrays (NCBI GEO accession GSE9113; ref. 28) revealed four tumors with deletions that included *FBXW7*, two of which were less focal than those we detected in WT (data not shown), whereas a recent report (29) also describes “discrete” deletions in T-cell acute lymphoblastic leukemia samples at this locus. These results suggest that *FBXW7* is targeted by both point mutations and deletions in tumor types in which it is commonly inactivated. No such deletions were detected when we examined publicly available data (GEO accession GSE12494; data not shown; ref. 30) from a large SNP array series derived from neuroblastoma, a tumor in which *FBXW7* point mutations have not been

described. Nevertheless, we have not yet ruled out the potential contribution to the tumor phenotype of deletion of the (2–7) immediately adjacent genes in our samples. Other loci on 4q may also be significant in WT. An earlier study (31) has reported loss of heterozygosity on 4q, including a region on 4q24–25 that does not overlap with *FBXW7*, whereas our own data on multiple genomic array platforms (data not shown) suggest that loss of the entire 4q chromosome arm is relatively frequent in WT.

The potential association between *FBXW7* status and histologic subtype we observed is intriguing. All three cases that had *FBXW7* aberrations but no mutations in the three other Wilms' tumor genes examined belonged to the relatively uncommon epithelial subtype and the association between histology and *FBXW7* status was significant. It may be relevant that the deletion of a single copy of *Fbxw7* in a *Tp53*-hemizygous mouse model results in a shift of the spectrum of observed malignancies toward tumors of epithelial tissues (26). The single tumor with mutations in *FBXW7*, *WT1*, and *CTNNB1* had stromal-type histology at nephrectomy. Mutations in both *WT1* and *CTNNB1* (frequently together, as here) have previously been associated with this histology (20–23). We may speculate that in situations in which both the *WT1/CTNNB1* and *FBXW7* axes are disrupted, the stromal phenotype associated with the former is dominant, overriding any tendency to develop epithelial predominance mediated by the latter. We also note that simultaneous mutation of *WT1* and *FBXW7* has recently been described in T-cell acute lymphoblastic leukemia (29), although the functional significance of this result is unclear, as the mutation frequencies of the two genes seem to be unrelated. The presence of a germline *FBXW7* mutation in the patient with aberrations in all three genes and an abnormality in the contralateral kidney raises the possibility that disruption of *FBXW7* may contribute to tumor predisposition. However, because one of the two *WT1* mutations in the tumor is also present in the germline, it is not possible to separate the potential contribution of *FBXW7* from the known role of *WT1*.

Earlier studies have reported *MYCN* gain or amplification in a few individual cases (32–34), although the data were too limited to test for potential associations with subtype. The present study is the first to analyze a WT series including a relatively large number of anaplastic tumors on a high-resolution SNP platform. Our finding of an association between *MYCN* gain and a high-risk histology in WT is in keeping with emerging evidence that elevated *MYCN* copy number, originally described in neuroblastoma (15) and used in risk stratification (16, 17), is associated with adverse outcome in other childhood tumors, including rhabdomyosarcoma (35) and medulloblastoma (36, 37). *MYCN* amplification is also observed in retinoblastoma (38), although existing data do not show a clinical correlation (39). Six of the nine patients in whose WT samples we detected *MYCN* gain suffered a relapse; five died. Two had intermediate risk mixed histology tumors and four had high-risk histology, including

one blastemal type and three anaplastic tumors. Samples from these three anaplastic cases had the highest levels of *MYCN* gain in the series; the three remaining anaplastic cases with *MYCN* aberrations had lower levels of gain and did not relapse. On histologic review, the three samples with the highest level of gain were found to have areas containing rhabdoid-like features on a background of diffuse anaplasia. When the detailed histology of all 12 UK anaplastic samples was reviewed, rhabdoid-like features were detected in two additional samples, one (with *MYCN* gain) from a patient who had not relapsed and the other (without *MYCN* gain) from a patient who had relapsed and died. A much larger WT series would be required to determine if *MYCN* gain in combination with anaplasia is associated with a significantly worse outcome than anaplasia alone or if the rhabdoid-like features that seemed more common in the subset of anaplastic tumors with *MYCN* gain are prognostically significant.

The current data for both genes are largely confined to European nephrectomy samples from patients treated under current SIOP protocols. These tumors have therefore been exposed to preoperative chemotherapy and represent histologic risk groups defined by their *in vivo* chemosensitivity (13). These groups have no direct equivalents in North American WT series from patients treated under Childhood Oncology Group protocols, who are typically chemo-naïve at resection. However, features such as anaplasia and the predominance of particular cell types (e.g., “epithelial predominance”) are recognized in individual immediate nephrectomy samples from Childhood Oncology Group patients. It would be interesting to conduct a similar analysis in samples drawn from a chemo-naïve series to determine if the apparent subtype specificity we have observed is restricted to classes defined by initial chemotherapy (in which additional mechanisms of selection for subclones carrying the aberrations we detected may operate) or is more broadly applicable to tumor classes characterized by specific histologic features, irrespective of chemotherapy.

Although genomic aberrations in *FBXW7* or *MYCN* are present in only a minority of tumors, other evidence suggests that mechanisms that affect pathways involving these genes are of more general importance in WT. Overexpression of *MYCN* is a recognized feature of WT (40–42) and its relative expression level has been identified as a significant clinical prognostic marker (43, 44). *FBXW7* is a component of an SCF (SKP1/CUL1/*FBXW7*) E3 ubiquitin ligase complex, which targets several key dominant proto-oncogene products for ubiquitination and subsequent proteasome-mediated degradation (27), with mutations leading to accumulation of its targets. It is therefore suggestive that the protein level of one of these targets, Cyclin E, has been shown to correlate with WT aggressiveness and metastasis (45). Intriguingly, *MYCN* itself was recently reported to be a direct target of the *FBXW7* SCF complex (46). This implies that the loss of *FBXW7* or gain of *MYCN* could have overlapping downstream effects, although the association of these alterations with different histologic

risk groups suggests a more complex picture. MYCN is only one of several known targets of FBXW7, so that disruption of the latter could perturb multiple pathways unaffected by copy number changes in the former. In addition, it is unclear if the dysregulation of MYCN levels by inactivation of FBXW7 would affect MYCN downstream targets to the same degree as direct copy number changes at the MYCN locus. The timing of mutational events and the broader pattern of concomitant genomic changes may also be significant. We detected FBXW7 aberrations in tumors with relatively stable genomes and in one case identified a germline change, features that suggest that disruption of this gene is a relatively early event. In contrast, the majority of MYCN gains were observed in anaplastic tumors with a background of widespread genomic disruption, features suggestive of a relatively late stage of tumor development.

Our results also have implications for the development of future therapeutic strategies. Although WT in general has an excellent response to treatment, anaplastic tumors that are metastatic at diagnosis or that recur remain largely intractable to current therapies. The genomic gain of a biomarker significantly associated with this high-risk histology, and with known oncogenic activity, therefore presents a potentially attractive target for novel treatment agents. Emerging therapies directed at MYCN function in other tumors, particularly neuroblastoma (47), could therefore be of significant clinical value. The link between the FBXW7 and MYCN pathways suggests further possibilities for in-

tervention. For example, the finding that AURKA, itself a known FBXW7 substrate, plays a critical role in sequestering MYCN from FBXW7-mediated degradation (46) highlights one class of interactions that could be targetable. As knowledge of these pathways continues to develop, so should the potential for more effective treatment of the WT patients with the poorest prognosis.

Disclosure of Potential Conflicts of Interest

No potential conflicts of interest were disclosed.

Acknowledgments

We thank the families, clinicians, and pathologists who contributed the samples used in this study to the Children's Cancer and Leukaemia Group Tumour Bank, United Kingdom, and the Paediatric Tumour Cell Bank of the Society of Paediatric Oncology and Haematology, Germany. We thank Clare Bedwell and Nick Bown, NHS Northern Genetics Service, Newcastle upon Tyne, for the MLPA analysis.

Grant Support

Cancer Research UK grant C1188/A4614, the Royal Marsden Hospital Children's Fund, and NHS funding to the NIHR Biomedical Research Centre.

The costs of publication of this article were defrayed in part by the payment of page charges. This article must therefore be hereby marked *advertisement* in accordance with 18 U.S.C. Section 1734 solely to indicate this fact.

Received 10/29/2009; revised 12/16/2009; accepted 01/07/2010; published OnlineFirst 03/23/2010.

References

- Hohenstein P, Hastie ND. The many facets of the Wilms' tumour gene, WT1. *Hum Mol Genet* 2006;15 Spec No 2:R196–201.
- Koesters R, Ridder R, Kopp-Schneider A, et al. Mutational activation of the β -catenin proto-oncogene is a common event in the development of Wilms' tumors. *Cancer Res* 1999;59:3880–2.
- Li CM, Kim CE, Margolin AA, et al. CTNNB1 mutations and overexpression of Wnt/ β -catenin target genes in WT1-mutant Wilms' tumors. *Am J Pathol* 2004;165:1943–53.
- Maiti S, Alam R, Amos CI, Huff V. Frequent association of β -catenin and WT1 mutations in Wilms tumors. *Cancer Res* 2000;60:6288–92.
- Royer-Pokora B, Weirich A, Schumacher V, et al. Clinical relevance of mutations in the Wilms tumor suppressor 1 gene WT1 and the cadherin-associated protein β 1 gene CTNNB1 for patients with Wilms tumors: results of long-term surveillance of 71 patients from International Society of Pediatric Oncology Study 9/Society for Pediatric Oncology. *Cancer* 2008;113:1080–9.
- Ruteshouser EC, Hendrickson BW, Colella S, Krahe R, Pinto L, Huff V. Genome-wide loss of heterozygosity analysis of WT1-wild-type and WT1-mutant Wilms tumors. *Genes Chromosomes Cancer* 2005;43:172–80.
- Rivera MN, Kim WJ, Wells J, et al. An X chromosome gene, WTX, is commonly inactivated in Wilms tumor. *Science* 2007;315:642–5.
- Ruteshouser EC, Robinson SM, Huff V. Wilms tumor genetics: mutations in WT1, WTX, and CTNNB1 account for only about one-third of tumors. *Genes Chromosomes Cancer* 2008;47:461–70.
- Ogawa O, Eccles MR, Szeto J, et al. Relaxation of insulin-like growth factor II gene imprinting implicated in Wilms' tumour. *Nature* 1993;362:749–51.
- Rainier S, Johnson LA, Dobry CJ, Ping AJ, Grundy PE, Feinberg AP. Relaxation of imprinted genes in human cancer. *Nature* 1993;362:747–9.
- Scott RH, Stiller CA, Walker L, Rahman N. Syndromes and constitutional chromosomal abnormalities associated with Wilms tumour. *J Med Genet* 2006;43:705–15.
- Bardeesy N, Falkoff D, Petrucci MJ, et al. Anaplastic Wilms' tumour, a subtype displaying poor prognosis, harbours p53 gene mutations. *Nat Genet* 1994;7:91–7.
- Vujanic GM, Sandstedt B, Harms D, Kelsey A, Leuschner I, de Kraker J. Revised International Society of Paediatric Oncology (SIOP) working classification of renal tumors of childhood. *Med Pediatr Oncol* 2002;38:79–82.
- Akhoondi S, Sun D, von der Lehr N, et al. FBXW7/hCDC4 is a general tumor suppressor in human cancer. *Cancer Res* 2007;67:9006–12.
- Schwab M, Alitalo K, Klempnauer KH, et al. Amplified DNA with limited homology to myc cellular oncogene is shared by human neuroblastoma cell lines and a neuroblastoma tumour. *Nature* 1983;305:245–8.
- Fischer M, Spitz R, Oberthur A, Westermann F, Berthold F. Risk estimation of neuroblastoma patients using molecular markers. *Klin Padiatr* 2008;220:137–46.
- Maris JM. The biologic basis for neuroblastoma heterogeneity and risk stratification. *Curr Opin Pediatr* 2005;17:7–13.
- Lingjaerde OC, Baumbusch LO, Liestol K, Glad IK, Borresen-Dale AL. CGH-Explorer: a program for analysis of array-CGH data. *Bioinformatics* 2005;21:821–2.
- Beroukhi R, Lin M, Park Y, et al. Inferring loss-of-heterozygosity from unpaired tumors using high-density oligonucleotide SNP arrays. *PLoS Comput Biol* 2006;2:e41.
- Corbin M, de Reynies A, Rickman DS, et al. WNT/ β -catenin pathway activation in Wilms tumors: a unifying mechanism with multiple entries? *Genes Chromosomes Cancer* 2009;48:816–27.
- Fukuzawa R, Heathcote RW, Sano M, Morison IM, Yun K, Reeve AE.

- Myogenesis in Wilms' tumors is associated with mutations of the WT1 gene and activation of Bcl-2 and the Wnt signaling pathway. *Pediatr Dev Pathol* 2004;7:125–37.
22. Schumacher V, Schneider S, Figge A, et al. Correlation of germ-line mutations and two-hit inactivation of the WT1 gene with Wilms tumors of stromal-predominant histology. *Proc Natl Acad Sci U S A* 1997;94:3972–7.
 23. Schumacher V, Schuhen S, Sonner S, et al. Two molecular subgroups of Wilms' tumors with or without WT1 mutations. *Clin Cancer Res* 2003;9:2005–14.
 24. Austinat M, Dunsch R, Wittekind C, Tannapfel A, Gebhardt R, Gaunitz F. Correlation between β -catenin mutations and expression of Wnt-signaling target genes in hepatocellular carcinoma. *Mol Cancer* 2008;7:21.
 25. Haruta M, Arai Y, Sugawara W, et al. Duplication of paternal IGF2 or loss of maternal IGF2 imprinting occurs in half of Wilms tumors with various structural WT1 abnormalities. *Genes Chromosomes Cancer* 2008;47:712–27.
 26. Mao JH, Perez-Losada J, Wu D, et al. Fbxw7/Cdc4 is a p53-dependent, haploinsufficient tumour suppressor gene. *Nature* 2004;432:775–9.
 27. Welcker M, Clurman BE. FBW7 ubiquitin ligase: a tumour suppressor at the crossroads of cell division, growth and differentiation. *Nat Rev Cancer* 2008;8:83–93.
 28. Mullighan CG, Miller CB, Radtke I, et al. BCR-ABL1 lymphoblastic leukaemia is characterized by the deletion of Ikaros. *Nature* 2008;453:110–4.
 29. Tosello V, Mansour MR, Barnes K, et al. WT1 mutations in T-ALL. *Blood* 2009;114:1038–45.
 30. Chen Y, Takita J, Choi YL, et al. Oncogenic mutations of ALK kinase in neuroblastoma. *Nature* 2008;455:971–4.
 31. Yuan E, Li CM, Yamashiro DJ, et al. Genomic profiling maps loss of heterozygosity and defines the timing and stage dependence of epigenetic and genetic events in Wilms' tumors. *Mol Cancer Res* 2005;3:493–502.
 32. McQuaid S, O'Meara A. N-myc oncogene amplification in paediatric tumours. *Ir J Med Sci* 1990;159:172–4.
 33. Norris MD, Brian MJ, Vowels MR, Stewart BW. N-myc amplification in Wilms' tumor. *Cancer Genet Cytogenet* 1988;30:187–9.
 34. Schaub R, Burger A, Bausch D, Niggli FK, Schafer BW, Betts DR. Array comparative genomic hybridization reveals unbalanced gain of the MYCN region in Wilms tumors. *Cancer Genet Cytogenet* 2007;172:61–5.
 35. Williamson D, Lu YJ, Gordon T, et al. Relationship between MYCN copy number and expression in rhabdomyosarcomas and correlation with adverse prognosis in the alveolar subtype. *J Clin Oncol* 2005;23:880–8.
 36. Aldosari N, Bigner SH, Burger PC, et al. MYCC and MYCN oncogene amplification in medulloblastoma. A fluorescence *in situ* hybridization study on paraffin sections from the Children's Oncology Group. *Arch Pathol Lab Med* 2002;126:540–4.
 37. Pfister S, Remke M, Benner A, et al. Outcome prediction in pediatric medulloblastoma based on DNA copy-number aberrations of chromosomes 6q and 17q and the MYC and MYCN loci. *J Clin Oncol* 2009;27:1627–36.
 38. Lee WH, Murphree AL, Benedict WF. Expression and amplification of the N-myc gene in primary retinoblastoma. *Nature* 1984;309:458–60.
 39. Corson TW, Gallie BL. One hit, two hits, three hits, more? Genomic changes in the development of retinoblastoma. *Genes Chromosomes Cancer* 2007;46:617–34.
 40. Nisen PD, Rich MA, Gloster E, et al. N-myc oncogene expression in histopathologically unrelated bilateral pediatric renal tumors. *Cancer* 1988;61:1821–6.
 41. Shaw AP, Poirier V, Tyler S, Mott M, Berry J, Maitland NJ. Expression of the N-myc oncogene in Wilms' tumour and related tissues. *Oncogene* 1988;3:143–9.
 42. Williams RD, Hing SN, Greer BT, et al. Prognostic classification of relapsing favorable histology Wilms tumor using cDNA microarray expression profiling and support vector machines. *Genes Chromosomes Cancer* 2004;41:65–79.
 43. Wittmann S, Wunder C, Zirn B, et al. New prognostic markers revealed by evaluation of genes correlated with clinical parameters in Wilms tumors. *Genes Chromosomes Cancer* 2008;47:386–95.
 44. Zirn B, Hartmann O, Samans B, et al. Expression profiling of Wilms tumors reveals new candidate genes for different clinical parameters. *Int J Cancer* 2006;118:1954–62.
 45. Berrebi D, Leclerc J, Schleiermacher G, et al. High cyclin E staining index in blastemal, stromal or epithelial cells is correlated with tumor aggressiveness in patients with nephroblastoma. *PLoS ONE* 2008;3:e2216.
 46. Otto T, Horn S, Brockmann M, et al. Stabilization of N-Myc is a critical function of Aurora A in human neuroblastoma. *Cancer Cell* 2009;15:67–78.
 47. Tonini GP, Pistoia V. Molecularly guided therapy of neuroblastoma: a review of different approaches. *Curr Pharm Des* 2006;12:2303–17.
 48. Browser tracks from <http://genome.ucsc.edu>.

Clinical Cancer Research

Subtype-Specific *FBXW7* Mutation and *MYCN* Copy Number Gain in Wilms' Tumor

Richard D. Williams, Reem Al-Saadi, Tasnim Chagtai, et al.

Clin Cancer Res 2010;16:2036-2045. Published OnlineFirst March 23, 2010.

Updated version	Access the most recent version of this article at: doi:10.1158/1078-0432.CCR-09-2890
Supplementary Material	Access the most recent supplemental material at: http://clincancerres.aacrjournals.org/content/suppl/2010/03/25/1078-0432.CCR-09-2890.DC1

Cited articles	This article cites 47 articles, 11 of which you can access for free at: http://clincancerres.aacrjournals.org/content/16/7/2036.full#ref-list-1
-----------------------	--

Citing articles	This article has been cited by 7 HighWire-hosted articles. Access the articles at: http://clincancerres.aacrjournals.org/content/16/7/2036.full#related-urls
------------------------	---

E-mail alerts	Sign up to receive free email-alerts related to this article or journal.
----------------------	--

Reprints and Subscriptions	To order reprints of this article or to subscribe to the journal, contact the AACR Publications Department at pubs@aacr.org .
-----------------------------------	--

Permissions	To request permission to re-use all or part of this article, use this link http://clincancerres.aacrjournals.org/content/16/7/2036 . Click on "Request Permissions" which will take you to the Copyright Clearance Center's (CCC) Rightslink site.
--------------------	--